Effect of alkaline additives over V-based catalysts supported on γ- Al_2O_3 for propane oxidative dehydrogenation

ABSTRACT

The olefins product are more reactive than the corresponding alkanes, and may easily be super-oxidised into CO and CO_2 in selective oxidation of alkanes. The proper balance of acid and base sites on the V-based catalyst surface plays a decisive role in limiting the complete oxidation of alkanes. Therefore, our goal was to evaluate the promoting effect of alkali metals and the support effect using boehmite as precursor for the propane oxidative dehydrogenation (ODH) reaction. Catalysts were prepared via co-impregnation of V and Na or K on a synthesized alumina support. The following characterization techniques were used: N_2 adsorption-desorption, X-ray diffraction (XRD), temperature programmed reduction (TPR) and isopropanol decomposition testes to evaluate the acid-base character. The catalyst performance in the propane ODH reaction was evaluated at the O_2:C_3H_8:He molar ratios of 5:2:4, 6:1:4, and 4:3:4. The K-doped catalysts exhibited higher propene selectivity owing to the modification of acid-base character that rendered the weaker interaction between olefinic intermediate and more basic catalyst surface. A high molar fraction of O_2 of the reaction mixture minimized coke formation and a high reoxidation rate possibly increased catalytic activity and propene selectivity.

Keywords: Propane oxidative dehydrogenation, alumina, V, Na, K

1. INTRODUCTION

Propene is one of the most important feedstocks in the petrochemical industry to produce mainly polypropylene, propylene oxide and acrylonitrile [1]. The main commercial processes for producing propene are steam cracking, fluid catalytic cracking (FCC) and catalytic dehydrogenation [2-4]. However, the capacity of the aforementioned processes to produce propene is limited, owing to their high-energy requirements and coke formation and so frequent catalytic regeneration is required. Catalytic dehydrogenation is a reversible reaction due to the hydrogen involved, and therefore the production of olefins is limited by thermodynamic equilibrium [4].

Recently, the growing global olefins demands has stimulated the search for environmental-friendly and exothermic processes for reducing energy costs [4,5]. In this scenario, propane oxidative dehydrogenation (ODH) has been pointed out as an alternative method for propene production that has the advantage of being an exothermic reaction; moreover it overcomes the thermodynamic restrictions of non-oxidative dehydrogenation owing to the formation of water ending the process. In addition, the use of O_2 in the reaction mixture minimizes the deposition of coke and ensures a long catalyst lifetime. However, the greatest challenge lies in obtaining selective catalysts that can inhibit the complete oxidation of olefins that leads to the formation of CO and CO_2 as by-products [5-7]. The propene yields reported in propane ODH reactions (less than 30%) are still not sufficient to satisfy economic feasibility [5].

Propane is a low-cost feedstock that can be found as a component of natural gas and it is easy to separate, making it a valuable but non-renewable gas. On the other hand, an emerging technology for the production of renewable “green” propane or bio-propane is gaining notoriety where it is already being operated on a large-scale production. Green propane has the potential to be produced from biomass, including as a side-product in the production of biodiesel, from glycerol and other substrates [8]. Therefore, there is a trend in the search for green and renewable routes to meet environmental concerns.

Boron-based catalysts have emerged as one of the most active and selective catalysts. The inhibition of the further dehydrogenation reaction of propene by a large energy barrier has revealed the cause of a high selectivity [9, 10]. On the other hand, the supported vanadium species are particularly one of the active components with redox properties of the greatest interest for hydrocarbons partial oxidation reactions; moreover, vanadium is a transition metal easily found in nature [11, 12]. The change in the oxidation state of vanadium during the propane ODH reaction has been better understood by the Mars-van-Krevelin (MVK) mechanism, which involves two steps [13, 14]:

(i) the reduction of V^{+5} to V^{+4} by the reaction of propane with catalyst oxygen, forming propene and water molecules;

(ii) the subsequent re-oxidation of the catalyst by O_2, completing the redox cycle V^{+5} / V^{+4}.

Recently, spectrometric measurements during the propane ODH reaction have allowed the identification of reaction intermediates to uncover reaction mechanisms. The most recent research findings are reported in paper published by Ternero-Hidalgo et al. (2021) [15]. The proposed mechanism was the propane activation, as the rate determining step in the reaction, that occurs via the irreversible formation of isopropoxide species, which can be desorbed as propylene or further oxidized to chemisorbed acetone. The latter can be converted into acetate ($CH3CHOO^-$) and formate ($CHOO^-$) species, which would be the precursors of CO_x. The propene formed during reaction can be adsorbed again on the surface and oxidized to isopropoxide species via neighboring V-OH groups such as Brønsted acid sites and continues with the subsequent steps for CO_x formation.

The use of CO_2 instead of O_2 has received considerable attention, as a mild oxidant, preventing deep oxidation, and consequently increasing the propene selectivity. Under these conditions, higher degree of reduction of vanadia species during the propane ODH reactions has been linked to higher selectivity [16, 17]. Nevertheless, the low olefin yield, poor catalyst stability and the demand for heating source due to the endothermic nature of the reactions constrain the CO_2-ODH process [17]. Therefore, the use of O_2 as an oxidant in this study was more appropriate, in addition to being an abundant and low-cost feedstock. Changes in the O_2:C_3H_8 molar ratio, also proposed in this study, can affect the reoxidation rate and, therefore, the ratio of the V^{5+}/V^{4+} species, and consequently, olefin selectivity [6, 7, 13].

Supported vanadium oxide catalysts are the conventional metal-based catalysts of the propane ODH reactions. However, its high reactivity deals with the formation of excess electrophilic oxygen species that increases the formation of CO and CO_2, decreasing the selectivity to propylene [5, 6]. The balance of acid and base sites on the V-based catalyst surface via the addition of alkaline and alkaline earth promoters has been a crucial parameter for propene selectivity control. The use of modifiers, such as alkali metals, can weaken the adsorption of propene on the less acidic and more basic surface of catalysts, avoiding the deep oxidation [18-20]. Teixeira-Neto el al. (2008) [21] studied the behavior of V-modified MCM-22 zeolite toward propane ODH reaction and noted that ion-exchange with

alkaline ions led to a decrease in cracking reactions, by removing the strong Brønsted acid sites. Furthermore, the changes in the physical-chemical and structural properties of different V-based catalysts have been studied for understanding the influence of promoters on catalytic performance [18, 22].

The support effect is also an important factor. The textural properties and lower acidity of Al_2O_3 than that of other oxides, such as TiO_2 and ZnO, has favored the dispersion of superficial V species [11]. The formation of isolated tetrahedral V^{5+} species seems to be the most suitable for higher propene selectivity [23]. For this reason, the use of alumina as an oxide support for V-containing catalysts for propane ODH reactions has provided higher propene selectivity [24-26]. Several methods can be used for the synthesis of aluminum hydroxide precursors, $Al(OH)_3$, or aluminum hydroxide oxides, AlO(OH), which generate transition alumina when it subjected to a heat treatment, [27, 28].

Our goal of this study was to evaluate the promoting effect of K and Na as additive and the effect support using boehmite as precursor to increase propene selectivity of the propane ODH reaction. The effect of changing acid-base properties, via alkali metals addition, on V-based catalyst activity was essentially evaluated. Unlike the use of commercial alumina, this work also proposed the synthesis of an efficient alumina for use as a support. The reaction conditions were taken into account, modifying the O_2/propane molar ratio of the reaction mixture.

2. MATERIAL AND METHODS

2.1 Synthesis

The aluminum hydroxide precursor was prepared using the precipitation method *via* the addition of $AlCl_3$ (pH = 0.5) into a NaOH solution (pH = 12.9), which was placed in a batch reactor at 65 °C under mechanical stirring until the pH was approximately 9.5. The obtained precipitate was washed with distilled water, dried, and calcined at 600 °C for 5 h to obtain the alumina support, which was denoted as Al_2O_3 (B). To synthesize alumina-supported V catalysts, the support was subjected to wet impregnation with excess solvent (water). Half-monolayer impregnation of 4 V atoms per square nanometer of alumina was performed by mixing a NH_4VO_3 solution heated to 70 °C and powder carrier in a vacuum rotary evaporator. Thereafter, the residual powder was dried and calcined at 450 °C for 5 h, and the prepared catalyst was denoted as 4V-Al (B). The alkali-metal-doped catalysts were prepared via the co-impregnation of V (half monolayer) and alkali metals (x = 0.5 and 1.0 Na or K atoms per square nanometer of support) on alumina. The doped catalysts were synthesized according to the aforementioned method using a mixture of NaOH or KOH aqueous solutions and NH_4VO_3 for co-impregnation. The prepared catalysts were denoted as 4V-xNa-Al (B) and 4V-xK-Al (B).

2.2 Physicochemical characterization

The specific surface areas and pore volume (Brunauer–Emmett–Teller method) and pore volume distribution (Barrett–Joyner–Halenda method) were determined using N_2 adsorption–desorption isotherms, which were obtained at -196 °C using a Belsorp-mini-II instrument. The samples were pretreated *in situ* under vacuum and were subsequently heated at 200 °C for 2 h.

X-ray diffraction (XRD) analyses were performed using a PANalytical Empyrean instrument with Cu Kα radiation (λ = 0,1544 nm) at a power of 30 kV, current of 20 mA, and goniometer angular velocity of 0.02º/s in the 2θ range of 10-80°.

Temperature programmed reduction (TPR) experiments were performed using a Quantachrome, ChemBET-3000 system equipped with a thermal conductivity detector (TCD). Samples (0.05 g) were dried *in situ* at 200 °C for 2 h under a He flow. Next, the solids were cooled to room temperature and reduced at 900 °C (temperature ramp of 10 °Cmin^{-1}) with a 5% H_2/N_2 mixture (flow rate of 30 mLmin^{-1}).

Isopropanol decomposition tests were performed at atmospheric pressure in a fixed-bed borosilicate glass reactor to evaluate the acid-base surface properties of the samples. The reactor was fed with isopropanol (99.7%), which was injected using a Thermo Separation Products P100 pump at a flow rate of 0.02 cm^{3}min^{-1} and was diluted with a He and N_2 mixture at a flow rate of 37.5 cm^{3}min^{-1}. The effluent gases were analyzed on line using a Varian 3380 chromatograph equipped with a TCD and a Poropak-Q column (4.5 m). The reaction was evaluated in the temperature range of 100-300 °C using 150 mg of catalysts and the residence time (W/F_{isop}) of 6.3 ghmol^{-1}. The conversion of isopropanol (X_{isop}), product selectivity (S_j), specific reaction rate (*SRR*), and the specific rate of product formation (*SRP*) were calculated as follows:

$$X_{isop}(\%) = \frac{\sum_j z_j n_j}{3n_{isop}+\sum_j z_j n_j}\ x\ 100 \quad (3)$$

$$S_j(\%) = \frac{z_j n_j}{\sum_j z_j n_j}\ x\ 100 \quad (4)$$

$$SRR = \frac{X_{isop}(\%)\ x\ F_{isop}}{W\ x\ S_g} \quad (5)$$

and

$$SRP = \frac{S_j(\%)\ x\ SRR}{S_g} \quad (6)$$

where n_{isop} is the number of moles of unconverted isopropanol in the product stream, n_j is the number of moles of gaseous carbon in product "j", z_j is the number of carbon atoms in gaseous carbon-containing product "j", F_{isop} is the reactor outflow of isopropanol, W is the catalyst weight, and S_g is the specific surface area.

2.3 Catalytic test

The catalytic activity of the prepared catalyst samples for the propane ODH reaction was tested at atmospheric pressure at a range temperature of 300-500 °C in a fixed-bed quartz microreactor (**Fig. 1**). The thermocouple placed inside the catalyst (0.15 g) was used to measure and control the temperatures and mass flow controller was used to control the gas flow (O_2, He and propane). The O_2:C_3H_8:He molar ratios were 5:2:4, 6:1:4, and 4:3:4 and the total flow rate was 48 ml.min^{-1}. The molar fraction of He and the total flow rate was maintained constant to determine the effect of the O_2:C_3H_8 molar ratio on the catalytic activity of the catalyst samples. The concentrations of unconverted propane and products were analyzed on line using a Varian 450 chromatograph equipped with a TCD using two 1/8" diameter columns. The stationary phases consisted of HS-N (80/100) and MS-13X (45/60).

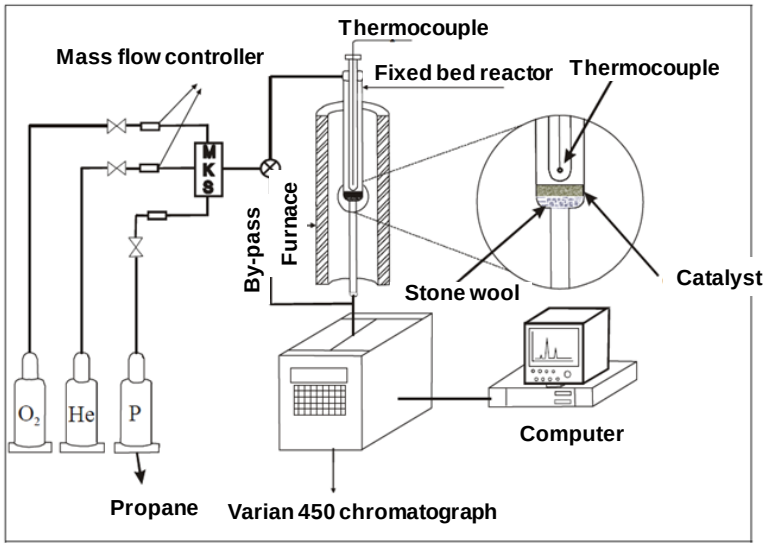

Fig. 1. Experimental set-up diagram of the propane ODH reaction

The performance of the catalysts was assessed using the conversion of propane (X_{C3H8}), product selectivity (S_i), and propene yield (Y_{C3H6}), which can be calculated as follows:

$$X_{C3H8}(\%) = \frac{\sum_i z_i n_i}{3n_{propane} + \sum_i z_i n_i} \; x \; 100 \tag{7}$$

$$S_i(\%) = \frac{z_i n_i}{\sum_i z_i n_i} \; x \; 100 \tag{8}$$

and

$$Y_{C3H6}(\%) = \frac{X_{C3H8}(\%) \; x \; S_{C3H6}(\%)}{100} \tag{9}$$

where $n_{propane}$ is the number of moles of unconverted propane in the product stream, n_i is the moles of gaseous carbon in the product "i", and z_i is the number of carbon atoms in the gaseous carbon-containing product "i". These equations were considered suitable for evaluating the performance of the catalysts because they provide accurate results, which depend on the reaction products measured using TCD analysis [29].

3. RESULTS AND DISCUSSION

3.1 Physicochemical characterization

The textural characteristics of the transition alumina and vanadium-and-alkali-metal-based catalysts are summarized in **Table 1**. The impregnation of vanadium oxide onto the alumina support caused a reduction in the values of the specific area (S_{BET}) and pore volume (V_P). The S_{BET} value decreased with increasing Na content. Conversely, S_{BET} increased with the addition of 1.0 K atom per square nanometer of alumina and can be attributed to the greater pore blockage caused by K^+ ions, whose ionic radius is higher that than of Na^+ ions.

Table 1. Specific area (S_{BET}), pore volume (V_P), and average pore radius (R_P) of alumina and respective catalysts

Support/ Catalysts	S_{BET} (m^2g^{-1})	V_P (cm^3g^{-1})	R_P (nm)
Al_2O_3 (B)	330	0.54	2.36
4V-Al (B)	176	0.27	3.12
4V-0.5Na-Al (B)	182	0.25	2.41
4V-1.0Na-Al (B)	169	0.24	2.41
4V-0.5K-Al (B)	159	0.26	3.12
4V-1.0K-Al (B)	180	0.25	2.41

Fig. 2 illustrates the N_2 adsorption-desorption isotherms of the samples. The undoped and alkali-metal-doped V catalysts (**Figure 2b-c**) and Al_2O_3 (B) support (**Figure 2a**) presented similar N_2 adsorption-desorption isotherms, which were type-IV isotherms with H-2 hysteresis loops according the IUPAC classifications, indicating that they had an ink-bottle mesoporous structure. In addition, the hysteresis loops length and pore volume decreased with addition of V and alkali metals, indicating the modification of texture properties.

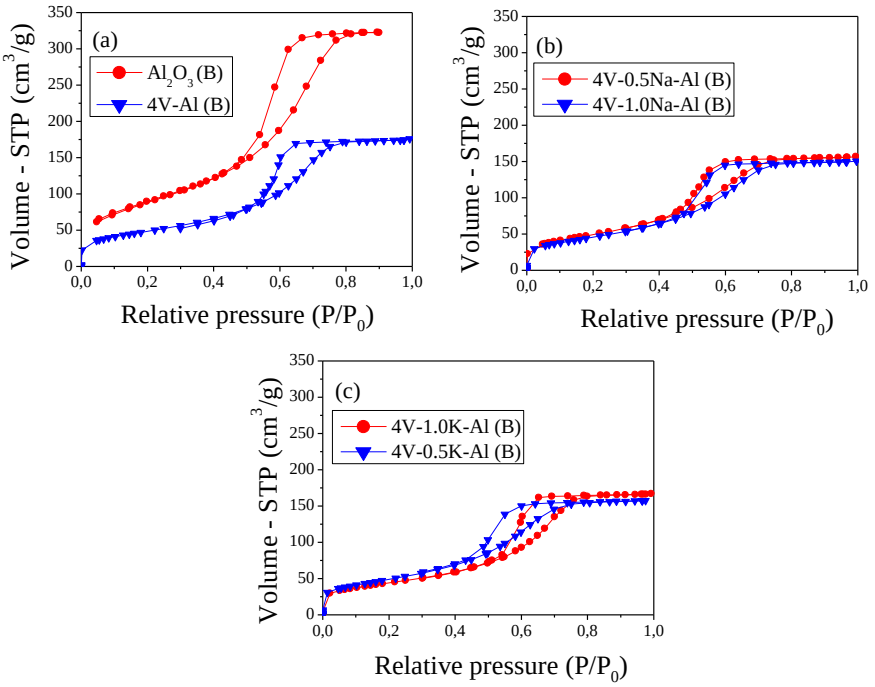

Fig. 2. N_2 adsorption-desorption isotherms of the Al_2O_3 (B) support and catalysts loaded with vanadium oxide and alkali metals

Fig. 3 presents the V_P distribution curves of the alumina and respective catalysts. The radius of most pores of the alumina support was between 1 and 3 nm (**Fig. 3a).** However, the V-based catalysts presented the radius of most pores between 1 and 5 nm (**Fig. 3b-d)**; possibly, the radius of pores increased because of the accommodation of V species and alkali metal ions into the pores.

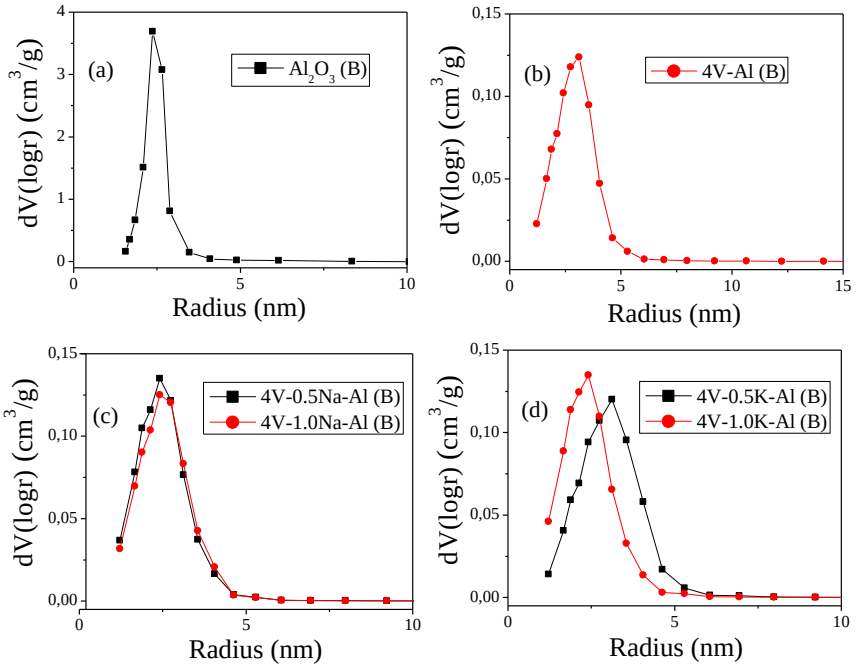

Fig. 3. V_p distribution curves of the Al_2O_3 (B) support and catalysts loaded with vanadium oxide and alkali metals

Fig. 4 shows the XRD profiles of the alumina support and catalysts. The alumina precursor presented orthorhombic aluminum hydroxide oxide (boehmite) structure (ICCD: 05-0190, 2θ = 13.46°, 28.08°, 38.58°, 49.1°, 64.94°, 71.90°). Upon calcination at 600 ° C, the boehmite precursor formed γ-Al_2O_3 (ICCD: 10-0425, 2θ = 46.12 °, 66.86 °), which presented low crystallinity. The XRD profiles of the catalysts impregnated with vanadium oxide and alkali metals were very similar to that of the alumina support. The absence of peaks related to bulk compounds indicated a good dispersion of superficial VO_x species. However, the formation of possible clusters of V nanoparticles (<4 nm), which are detectable by spectroscopic analysis, such as Raman and UV-Vis, could not be ruled out [29, 30], although the total V + K or V + Na coverage was below a monolayer. Furthermore, the dispersion of vanadium oxide depends on the textural properties, concentration of surface hydroxyl groups of oxide support for anchoring V species, synthesis methods and vanadium precursors [5, 12]. For us, the purpose of catalyst synthesis was achieve a better dispersion of V species for a half-monolayer, which are possibly the most selective for propane oxidative dehydrogenation reactions.

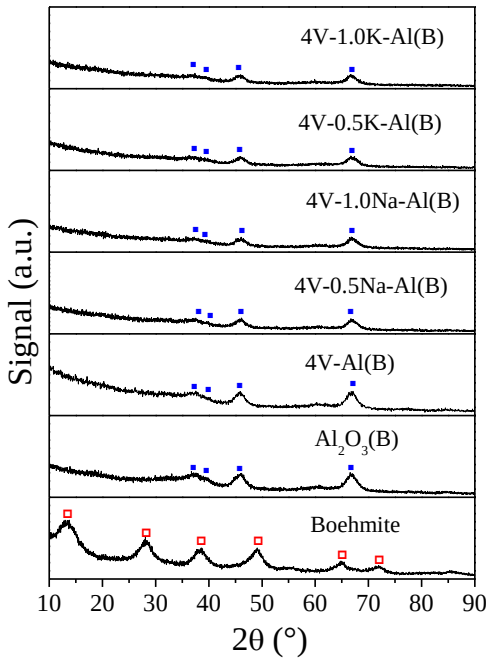

Fig. 4. X-ray diffractograms of catalyst samples. The ☐ and ■ peaks represent gibbsite and χ-Al_2O_3 phases, respectively

The TPR profiles of the catalysts are presented in **Fig. 5**. The undoped V catalyst exhibited a single reduction temperature peak (532 °C), which corresponded to the reduction of V_2O_5 to V_6O_{13}. However, the same reduction peak shifted to higher temperatures (538-557 °C) for doped V catalysts that indicated a decrease in reducibility, owing to the higher inhibition of vanadium active sites by the alkali metal ions [19]. A second reduction peak emerged at 570 °C for 4V-0.5K-Al (B) catalyst, which could be associated with the formation of vanadium oxide aggregates that were caused by less dispersion of surface V species or compounds that were formed between potassium and vanadium.

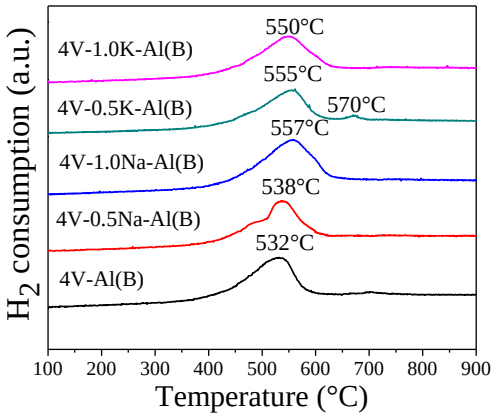

Fig. 5. Temperature programmed reduction curve of the catalysts

The SRR and SRP values for the decomposition of isopropanol at 280 and 300 °C are summarized in **Tables 2** and **3**, respectively. For the evaluation of acid-base properties, the product distribution was analyzed according to the nature of surface sites. The formation of propene via isopropanol dehydration requires the presence of Lewis or Brønsted acid sites, whereas the formation of acetone via isopropanol dehydrogenation occurs at basic or redox sites. Diisopropyl ether are formed via intermolecular dehydration at strong and medium strength Lewis sites and basic sites [31, 32]. The addition of V to alumina support increased substantially the catalytic activity and propene production. The high propene SRP and onset of acetone formation indicated the strong acid and redox character of V species. In contrast, the addition of alkali metals led to a decrease in SRR and propene SRP, being proportional to alkali metal content of the catalysts. The inhibition of acid sites by K was more pronounced that of Na, because the ionic radius of K^+ is higher than that of Na^+. The acetone production, which occur preferentially at basic sites, increased for the doped catalysts. Only traces of diisopropyl ether were observed during the tests.

Table 2. Specific reaction rate (SRR) and specific rate of product formation (SRP) of the support and catalysts at 280 °C

Support/ Catalysts	SRR ($\mu molm^{-2}min^{-1}$)	SRP ($\mu molm^{-2}min^{-1}$)	
		Propene	Acetone
Al_2O_3 (B)	1.71	1.71	0.01
4V-Al (B)	16.1	14.3	4.21
4V-0.5Na-Al (B)	12.7	10.4	5.85
4V-1.0Na-Al (B)	10.7	7.4	5.72
4V-0.5K-Al (B)	10.4	6.9	5.96
4V-1.0K-Al (B)	6.72	4.1	5.89

Table 3. Specific reaction rate (SRR) and specific rate of product formation (SRP) of the support and catalysts at 300 °C

Support/ Catalysts	SRR ($\mu molm^{-2}min^{-1}$)	SRP ($\mu molm^{-2}min^{-1}$)	
		Propene	Acetone
Al_2O_3 (B)	4.4	4.4	-
4V-Al (B)	30.9	27.3	3.8
4V-0.5Na-Al (B)	25.9	22.1	4.6
4V-1.0Na-Al (B)	21.3	15.7	5.4
4V-0.5K-Al (B)	20.8	14.5	6.1
4V-1.0K-Al (B)	15.3	9.9	5.3

3.2 Catalytic test

Fig. 6 shows the catalytic performance of the undoped and alkali-metal-doped V catalysts for the propane ODH reaction at the O_2:C_3H_8:He molar ratio of 5:2:4. The highest propene yields were observed at the beginning of the experiments (300 °C) for all catalysts (**Fig. 6b**). In contrast, the propane conversion increased (**Fig. 6a**) and propene yield decreased at higher temperature (500 °C) owning to the olefin combustion process to form CO and CO_2. However, the propane conversion at 300 °C and 500°C decreased with the addition of alkali metals, because of the effect of the dopants on the redox properties of V. Furthermore, a certain number of propane adsorption centers were blocked by the alkali metal ions, affecting reagent accessibility [33].

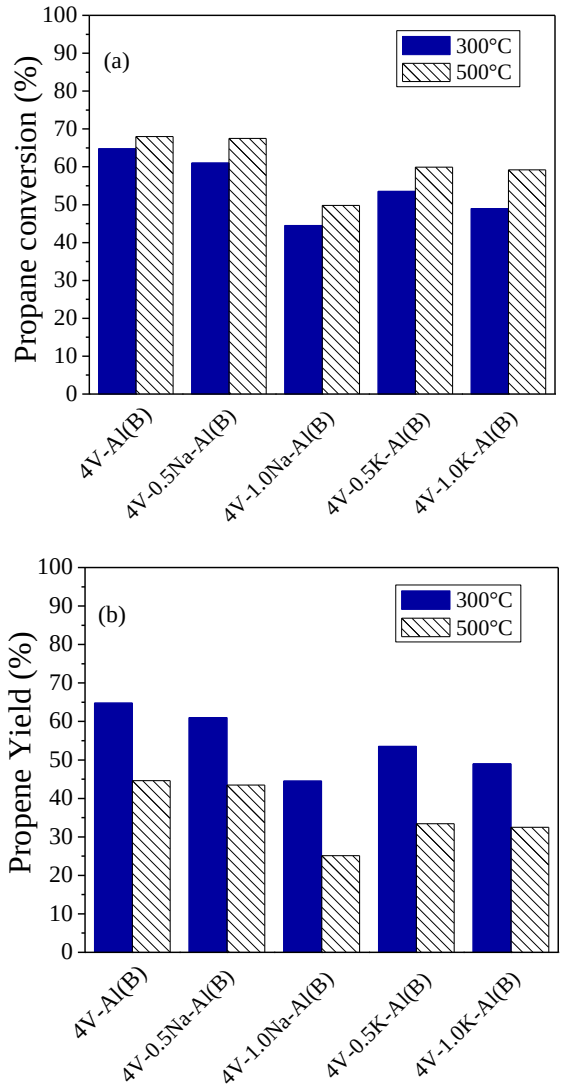

Fig. 6. Propane conversion (a) and propene yield (b) of the catalysts during propane oxidative dehydrogenation

The start of the combustion processes is depicted in **Table 4**. The production of CO_x over the alkali-metal-doped catalysts started at higher temperatures than that of the undoped catalyst. These results were attributed to the alkali metal ions blocking the strong acid and nonselective sites that favor the formation of CO_x [19]. This effect was more significant for the K-doped catalysts because of the ion radius of K^+ being larger than that of Na^+. The higher inhibition of the acidic sites by K is confirmed by the lowest propylene production, since propylene production during the isopropanol decomposition reaction require the presence of acid sites.

Table 4. Catalytic activity for the propane oxidative dehydrogenation reaction

Catalysts	Initial propane conversion (%)	Initial propene yield[a] (%)	Initial combustion temperature (°C)
4V-Al (B)	64.8	64.8	322
4V-0.5Na-Al (B)	61	61	356
4V-1.0Na-Al (B)	44.5	44.5	357
4V-0.5K-Al (B)	53.4	53.4	380
4V-1.0K-Al (B)	49	49	370

[a]The highest propene yields were observed at the beginning of the reactions

Fig. 7 presents the comparison of propene selectivity in the propane ODH reaction at 420 °C, in which the difference in selectivity among the catalysts was more noticeable. The results showed an improvement in propene selectivity with the addition of alkali metals, and the 4V-0.5K-Al (B) catalyst was more selective than the other alkali-metal-doped catalysts. The acetone production, which occur at basic sites, during the isopropanol decomposition test, was higher for 4V-0.5K-Al (B) catalyst and their pronounced increase in basicity could have allowed an easier desorption of propene from the less acidic surface, preventing consecutive propene combustion to CO and CO_2 [18]. The electronic density caused by K^+ ions in the V–O active center was greater than that of Na^+ ions, rendering the K-doped catalysts less acidic than the Na-doped catalysts at the same Na and K content [34]. However, the basicity decreased with increasing K content and the 4V-1.0K-Al (B) catalyst could not have provided a better desorption of propene than the 4V-0.5 K-Al (B) catalyst.

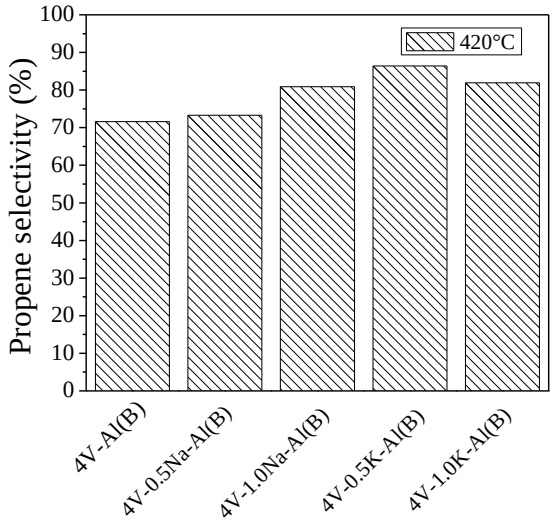

Fig. 7. Propene selectivity during propane oxidative dehydrogenation

Fig. 8 illustrates the catalytic performance of the most selective catalyst, 4V-0.5K-Al (B), using the O_2:C_3H_8:He molar ratios of 6:1:4, 5:2:4 and 4:3:4; the molar fraction of He and total flow rate were maintained constant. The catalytic activity of the 4V-0.5K-Al (B) catalyst increased with increasing O_2 molar fraction, as demonstrated by the increase in propane conversion (**Fig. 8a**) and propene yield (**Fig.8b**) at 300 °C and 500 °C. The high olefin yield can be attributed to the interactions of propane molecules with a large number of oxygen

active sites restored to the catalytic structure that were sufficient to selectively convert propane to propylene [6]. Conversely, the catalytic performance decreased when the molar fraction of O_2 was lower (O_2:C_3H_8:He = 4:3:4); catalytic activity and propene yield decreased owing to a possible insufficient O replacement in the catalytic structure [6]. Moreover, at the O_2:C_3H_8:He molar ratio of 4:3:4, catalyst deactivation increased with the coke formation, in that the catalyst samples appeared blackened after the catalytic test. Therefore, O_2 played an important role for preventing the deposition of coke on the catalyst surface [7] with increasing O_2 molar fraction.

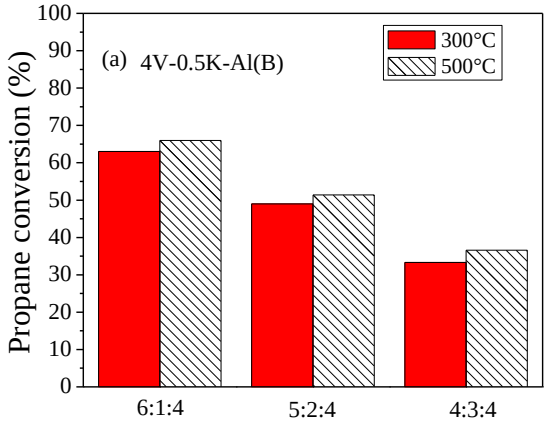

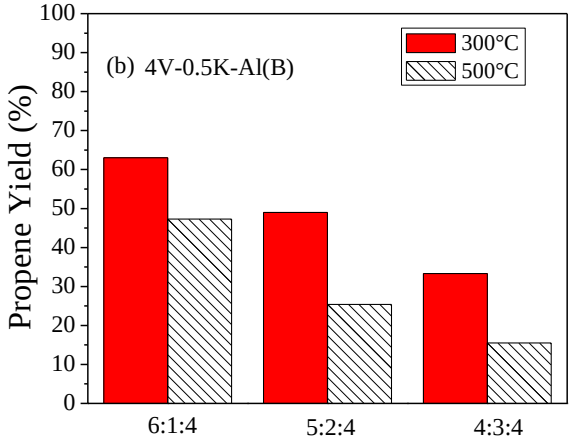

Fig. 8. Propane conversion (a) and propene yield (b) of the 4V-0.5K-Al (B) catalyst at different O_2:C_3H_8:He molar ratios

The propene selectivity curves of the 4V-0.5K-Al(B) catalyst at different O_2:C_3H_8:He molar ratios are presented in **Fig 9**. The increase in O_2 molar fraction improved the propylene selectivity. Some studies have reported a greater reduction of V cations with decreasing amount of O_2, which favored selectivity to olefins [6, 7, 35-37]. In this specific study, however, a higher O_2 molar fraction facilitated catalytic regeneration, providing an increase

in propene yield and decreased production of CO and CO_2. Therefore, the propene selectivity depends on the oxygen/alkane feeding ratios and the composition and physicochemical properties of the prepared catalysts during the catalytic test usually carried out at atmospheric pressure. Thus, the O_2:C_3H_8:He molar ratio of 6:1:4 was the most suitable for the propene ODH reaction.

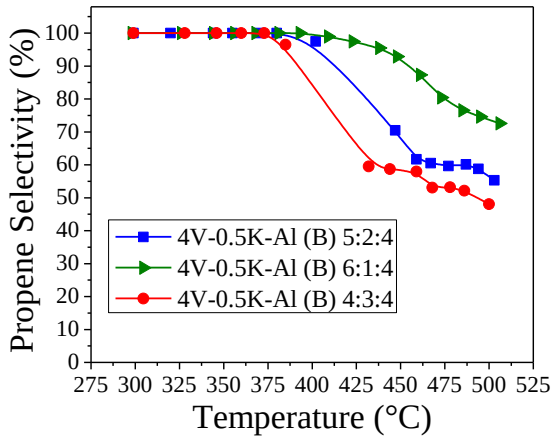

Fig. 9. Propene selectivity of the 4V-0.5K-Al (G) catalyst at different O_2:C_3H_8 molar ratios

Higher reaction temperatures may promote the adsorption of oxygen on the surface of catalysts, and therefore higher rates of re-oxidation may have favored the increase in propane conversion (**Fig. 6a** and **Fig. 8a**) [38]. However, higher reaction temperatures favored the undesired reactions that decreased the propene selectivity (**Fig. 9**).

The alkali metal dopants have been reported to improve propene selectivity but have been associated with a decrease in catalytic activity and can be attributed to the alkali metal ions blocking the strong acid and nonselective sites [18, 19]. The catalysts prepared in this study presented same behavior, with the important contribution of alkali metals and O_2 in the selectivity to propylene.

4. CONCLUSION

The precipitation method was satisfactory, since the synthesized alumina support presented specific area and pore volume suitable for the dispersion of surface V species; the XRD analyzes did not indicate the significant agglomeration of such species. The change in acid-base properties with the addition of potassium, as a promoter, provided better propene selectivity and can be attributed to the weak interaction between the olefinic intermediates and more basic catalyst surface. The change in C_3H_8:O_2 molar ratios during the propane ODH tests revealed the importance of the availability of oxygen of the reaction mixture for replacement in the catalytic structure and prevention of coke formation. The 4V-0.5K-Al (B) catalyst was the most selective (high initial conversion of propane of approximately 63% at 300 °C and the O_2:C_3H_8:He molar ratio of 6:1:4) eliminating the complete oxidation to CO and CO_2. The performance of the K-doped catalysts was superior to previously published results [18, 19, 39, 40] in that the combustion process were partially inhibited with the presence of the alkali metal promoters. Therefore, further detailed studies should be performed to elucidate the interactions of alkali metals with support materials prepared in

this paper and the influence of O_2:C_3H_8 molar ratio for a promising catalytic efficiency.

ACKNOWLEDGEMENTS

This study was financed in part by the Coordenação de Aperfeiçoamento de Pessoal de Nível Superior, Brazil (CAPES), Finance Code 001.

COMPETING INTERESTS

Authors have declared that no competing interests exist.

REFERENCES

1. Plotkin JS. The Changing Dynamics of Olefin Supply/Demand**.** Catal. Today. 2005: 106(1-4):10-14. https://doi.org/10.1016/j.cattod.2005.07.174
2. Amghizar I, Vandewalle LA, Van Geem KM, Marin GB. New Trends in Olefin Production. Engineering. 2017:3(2):171-178. https://doi.org/10.1016/J.ENG.2017.02.006
3. Alotaibi FM, González-Cortés S, Alotibi MF, Xiao T, Al-Megren H, Yang G, Edwards PP. Enhancing the production of light olefins from heavy crude oils: Turning challenges into opportunities. Catal. Today. 2018:317:86-98. https://doi.org/10.1016/j.cattod.2018.02.018
4. Cavani F, Ballarini N, Cericola A. Oxidative Dehydrogenation of Ethane and Propane: How far from Commercial Implementation? Catal. Today. 2007:127(1-4):113-131. http://doi.org/10.1016/j.cattod.2007.05.009
5. Carrero CA, Schloegl R, Wachs IE, Schomaecker R. Critical Literature Review of the Kinetics for the Oxidative Dehydrogenation of Propane over Well-Defined Supported Vanadium Oxide Catalysts. ACS Catal*.* 2014:4(10):3357-3380. https://doi.org/10.1021/cs5003417
6. Al-Ghamdi SA, de Lasa HI. Propylene Production via Propane Oxidative Dehydrogenation over VO_x/γ-Al_2O_3 Catalyst. Fuel. 2014:128:120-140. https://doi.org/10.1016/j.fuel.2014.02.033
7. Mamedov EA, Corberán VC. Oxidative Dehydrogenation of Lower Alkanes on Vanadium Oxide-based Catalysts. The Present State of the Art and Outlooks. Appl. Catal. A Gen. 1995:127(1-2):1-40. https://doi.org/10.1016/0926-860X(95)00056-9
8. Carter JH, Bere T, Pitchers JR, Hewes DG, Vandegehuchte BD, Kiely CJ, Taylor SH, Hutchings GJ. Direct and oxidative dehydrogenation of propane: from catalyst design to industrial application. Green Chem. 2021:23:9747-9799. https://doi.org/10.1039/D1GC03700E
9. Chaturbedy P, Ahamed M, Eswaramoorthy M. Oxidative Dehydrogenation of Propane over a High Surface Area Boron Nitride Catalyst: Exceptional Selectivity for Olefins at High Conversion. ACS Omega. 2018:3:369−374. https://doi.org/10.1021/acsomega.7b01489
10. Si C, Lian Z, Olanrele SO, Sun XY, Li B. Revealing the origin of the reactivity of metal-free boron nitride catalysts in oxidative dehydrogenation of propane. Appl. Surf. Sci. 2020:519:146241. https://doi.org/10.1016/j.apsusc.2020.146241
11. Blasco T, Nieto JML. Oxidative Dehydrogenation of Short Chain Alkanes on Supported Vanadium Oxide Catalysts. Appl. Catal. A Gen.1997:157(1-2):117-142.https://doi.org/10.1016/S0926-860X(97)00029-X.

12. Weckhuysen BM, Keller DE. Chemistry, Spectroscopy and the Role of Supported Vanadium Oxides in Heterogeneous Catalysis. Catal. Today. 2003:78(1-4):25-46. https://doi.org/10.1016/S0920-5861(02)00323-1
13. Chu W, Luo J, Paul S, Liu Y, Khodakov A, Bordes E. Synthesis and Performance of Vanadium-based Catalysts for the Selective Oxidation of Light Alkanes. Catal. Today. 2017:298:145-157. https://doi.org/10.1016/j.cattod.2017.05.004
14. Redfern PC, Zapol P, Sternberg M, Adiga SP, Zygmunt SA, Curtiss LA. Quantum Chemical Study of Mechanisms for Oxidative Dehydrogenation of Propane on Vanadium Oxide. J. Phys. Chem. B. 2006:110(16):8363-8371. https://doi.org/10.1021/jp056228w
15. Ternero-Hidalgo JJ, Daturi M, Clet G, Bazin P, Bañares MA, Portela R, Guerrero-Pérez MO, Rodríguez-Mirasol J, Cordero T. A simultaneous operando FTIR & Raman study of propane ODH mechanism over V-Zr-O catalysts. Catal. Today. 2021: *in press*. https://doi.org/10.1016/j.cattod.2021.06.012
16. Rogg S, Hess C**.** CO_2 as a soft oxidant for propane oxidative dehydrogenation: A mechanistic study using *operando* UV Raman spectroscopy. J. CO2 Util. 2021:50:101604. https://doi.org/10.1016/j.jcou.2021.101604
17. Gambo Y, Adamu S, Tanimu G, Abdullahi IM, Lucky RA, Ba-Shammakh MS, Hossain MM. CO_2-mediated oxidative dehydrogenation of light alkanes to olefins: Advances and perspectives in catalyst design and process improvement. Appl. Catal. A Gen. 2021:623:118273. https://doi.org/10.1016/j.apcata.2021.118273
18. Cortez GG, Fierro JLG, Bañares MA. Role of Potassium on the Structure and Activity of Alumina-supported Vanadium Oxide Catalysts for Propane Oxidative Dehydrogenation. Catal. Today. 2003:78(1-4):219-228. https://doi.org/10.1016/S0920-5861(02)00341-3
19. Lemonidou AA, Nalbandian L, Vasalos IA. Oxidative Dehydrogenation of Propane over Vanadium Oxide based Catalysts. Effect of Support and Alkali Promoter. Catal. Today, 2000:61(1-4):333-341. https://doi.org/10.1016/S0920-5861(00)00393-X
20. Putra MD, Al-Zahrani SM, Abasaeed AE. Kinetics of oxidehydrogenation of propane over alumina-supported Sr–V–Mo catalysts. Catal. Commun. 2012:26:98–102. https://doi.org/10.1016/j.catcom.2012.04.018
21. Teixeira-Neto AA, Marchese L, Landi G, Lisi L, Pastore HO. [V,Al]-MCM-22 catalyst in the oxidative dehydrogenation of propane. Catal. Today. 2008: 133–135: 1–6. https://doi.org/10.1016/j.cattod.2007.11.012
22. Grant JT, Love AM, Carlos A, Carrero CA, Huang F, Panger J, Verel R, Hermans I. Improved Supported Metal Oxides for the Oxidative Dehydrogenation of Propane. Top. Catal. 2016:59:1545-1553. https://doi.org/10.1007/s11244-016-0671-2
23. Rossetti I, Mancini GF, Ghigna P, Scavini M, Piumetti M, Bonelli B, Cavani F, Comite A. Spectroscopic Enlightening of the Local Structure of VO_X Active Sites in Catalysts for the Odh of Propane. J. Phys. Chem. C. 2012:116(42):22386-22398. https://doi.org/10.1021/jp307031b
24. Martra G, Arena F, Coluccia S, Frusteri F, Parmaliana A. Factors controlling the selectivity of V_2O_5 supported catalysts in the oxidative dehydrogenation of propane. Catal. Today. 2000:63(2-4):197-207. https://doi.org/10.1016/S0920-5861(00)00460-0
25. Khodakov A, Olthof B, Bell AT, Iglesia E. Structure and Catalytic Properties of Supported Vanadium Oxides: Support Effects on Oxidative Dehydrogenation Reactions. J. Catal. 1999:181(2):205-216. https://doi.org/10.1006/jcat.2002.3570
26. Arena, F, Frusteri, F, Parmaliana, A. How oxide carriers affect the reactivity of V_2O_5 catalysts in the oxidative dehydrogenation of propane. Catal. Letters. 1999:60: 59-63. https://doi.org/10.1023/A%3A1019074016773
27. Jiao WQ, Yue MB, Wang YM, He MY. Synthesis of morphology-controlled mesoporous transition aluminas derived from the decomposition of alumina

hydrates. Microporous and Mesoporous Materials. 2012:147(1):167-177. https://doi.org/10.1016/j.micromeso.2011.06.012
28. Busca G. The surface of transitional aluminas: A Critical Review. Catalysis Today 2014; 226: 2-13. https://doi.org/10.1016/j.cattod.2013.08.003
29. Carrero CA, Keturakis CJ, Orrego A, Schomäcker R, Wachs IE. Anomalous reactivity of supported V_2O_5 nanoparticles for propane oxidative dehydrogenation: influence of the vanadium oxide precursor. Dalton Trans. 2013:42:12644-12653. https://doi.org/10.1039/C3DT50611H
30. Wachs IE, Roberts CA. Monitoring surface metal oxide catalytic active sites with Raman spectroscopy. Chem. Soc. Rev. 2010:39:5002-5017. https://doi.org/10.1039/C0CS00145G
31. Gervasini A, Fenyvesi J, Aurox A. Study of the acidic character of modified metal oxide surfaces using the test of isopropanol decomposition. Catal. Letters. 1997:43: 219-228. https://doi.org/10.1023/A:1018979731407
32. Bedia J, Rosas JM, Vera D, Rodríguez – Mirasol J, Cordero T. Isopropanol decomposition on carbon based acid and basic catalysts. Catal. Today. 2010:158(1-2), 89-96. https://doi.org/10.1016/j.cattod.2010.04.043
33. Słoczyński J. Kinetics and mechanism of reduction and reoxidation of the alkali metal promoted vanadia-titania catalysts. Appl. Catal. A Gen. 1996:146(2):401-423. https://doi.org/10.1016/S0926-860X(96)00172-X
34. Grzybowska-Swierkosz B. Effect of Additives on the Physicochemical and Catalytic Properties of Oxide Catalysis in Selective Oxidation Reactions. Top. Catal. 2002:21:35-46. https://doi.org/10.1023/A:1020547830167
35. Høj M, Jensen AD, Grunwaldt JD. Structure of Alumina Supported Vanadia Catalysts for Oxidative Dehydrogenation of Propane prepared by Flame Spray Pyrolysis. Appl. Catal. A Gen. 2013:451:207-215. https://doi.org/10.1016/j.apcata.2012.09.037
36. Cortez GG, Bañares MA. A Raman Spectroscopy Study of Alumina-Supported Vanadium Oxide Catalyst during Propane Oxidative Dehydrogenation with Online Activity Measurement. J. Catal. 2002:209(1):197-201. https://doi.org/10.1006/jcat.2002.3600
37. Murgia V, Sham E, Gottifredi JC, Farfan Torres EM. Oxidative dehydrogenation of propane and n-butane over alumina supported vanadium catalysts. Lat. Am. Appl. Res. 2004:34:75-82.
38. Wu T, Yu Q, Wang K, Annaland MS. Development of V-Based Oxygen Carriers for Chemical Looping Oxidative Dehydrogenation of Propane. Catalyst. 2021:11:119. https://doi.org/10.3390/catal11010119
39. Galli A, López Nieto JM, Dejoz A, Vazquez MI. The effect of potassium on the selective oxidation of *n*-butane and ethane over Al_2O_3-supported vanadia catalysts. Catal. Lett. 1995:34:51-58. https://doi.org/10.1007/BF00808321
40. Ermini V, Finocchio E, Sechi S, Busca G, Rossini S. Propane oxydehydrogenation over alumina-supported vanadia doped with manganese and potassium. Appl. Catal. A Gen. 2000:198(1-2):67-79. https://doi.org/10.1016/S0926-860X(99)00499-8